Lupane Derivatives: Design, Isolation, Synthesis and anti-malarial activity against *Plasmodium falciparum* 3D7 strains.

Pierre Yemback
  University of Yaounde I: Universite de Yaounde I

Eyong Kenneth Oben (✉ eyongkk@yahoo.com)
  University of Yaounde I: Universite de Yaounde I

Noella Efange
  University of Buea

Michael HK Kamdem
  University of Johannesburg

Dereck T Ndinteh
  University of Johannesburg

Patricia O Odumosu
  University of Jos

Gabriel N Folefoc
  University of Yaounde I: Universite de Yaounde I

Lawrence Ayong
  Centre Pasteur du Cameroun

Thomas Werner
 University of Paderborn: Universitat Paderborn

Abstract

To search for leads against malaria, compounds from the Cameroon Natural Product Library (CANAPL), were screened by molecular docking studies against the enzyme target Glyceraldehyde-3-phosphate dehydrogenase (PfGAPDH) for *Plasmodium falciparum*. Amongst these docking hits were the lupeol cinnamate (1) and oleanane cinnamate (2). Triterpenoids with structural similarities to (1) and (2) were isolated from *Baillonella toxisperma* (Pierre); olean-12-en-3β-hexadecanoate (3), 3-β-trans cinnamoyloxylup-20(29)-ene (4), oleanoic acid benzoate (5), 3β-amyrin (6), taraxerol (7), betulonic acid (8), β-sitosterol (9), betulinic acid (10), 3β-(trans-p-Coumaroyl)oxylup-20(29)-en-28-oïc acid (11), and screened alongside Betuline (12) and oleanolic acid (13). The favorable compounds 8 and 11 with 100% growth inhibition on *Plasmodium falciparum* 3D7 strains together with compounds 4, 10 and 12 were structurally optimized to afford new lupane derivatives with the privilege α-β unsaturated carbonyl medicinal scaffolds; betulonic acid acryl aldehyde (14), betulin acryl aldehyde (15), 3β-(*trans-p*-Coumaroyl)oxylup-20(29)-en-28-oïc acid acryl aldehyde (16), betulinic acid acryl aldehyde (18) and 3-β-*trans* cinnamoyloxylup-20(29)-ene acryl aldehyde (19) exhibiting more potent anti-malarial activities with IC_{50} values of 0.703 µM, 2.15 µM, 1.28 µM, and 3.79 µM for compounds 14, 15, 16 and 18 respectively. The modified compounds with the privilege α, β-unsaturated carbonyl medicinal scaffolds could be further optimized into potent antimalarial agents.
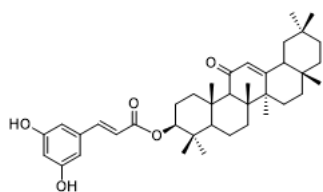
Introduction

Global mapping data indicate that malaria continues to be a major challenge with about 3.3 billion people at risk of exposure [1, 2]. The 2021 WHO report reveals that about 241 million people are infected with about 627 000 deaths [3]. The eradication of malaria through the development of new insecticides, mosquito vector disruptions through more hygienic environment and the development of new antimalarial therapeutic agents remain a major priority worldwide. Despite the existence of effective antimalarial drugs such as artemisinin and chloroquine, increasing parasite resistance to these drugs is a major reason for the continuous search of cost-effective and new analogues with novel modes of action [4, 5].

Malaria is a disease caused by parasites of the genus *Plasmodium*, with *P. falciparum* being the most pathogenic and attacks red bloods cells. The absence of a durable Krebs cycle in these parasites and the sole dependence on glycolysis for energy needs makes glycolytic pathway enzymes potential targets for antimalarial chemotherapies [6, 7]. Glyceraldehyde 3-phosphate dehydrogenase (abbreviated as *Pf*GAPDH for *Plasmodium falciparum*) is a key glycolytic enzyme that catalyzes the conversion of Glyceraldehyde 3-phosphate (G3P) into 1,3-bisphosphate glycerate (1,3-BPG), with the concomitant reduction of nicotinamide adenine dinucleotide (NAD^+) to NADH [8]. This is the 6th step in the glycolytic breakdown of glucose, an important pathway of energy and carbon molecule supply which takes place in the cytosol of eukaryotic cells [9].

The molecular docking analysis can provide an important view into ligand-enzyme bindings and conformations [10]. In order to explore the potential inhibitors of the PfGAPDH, a molecular docking analysis was performed on a current collection of 4000 compounds from CANAPL (CAmeroonian NAtural Products Library); a database of compounds isolated from Cameroonian medicinal plants from the Department of Organic Chemistry of the University of Yaounde 1. These compounds were docked into the active site of PfGAPDH (PDB code: 1ywg). The best results show that the lupane 1 and oleanane 2 derivatives were the most promising and exhibited binding energy (-10.55 and – 10.51 kcal/mol) compared to PfGAPDH inhibitors; heptelidic acid (-6.47 kcal/mol), iodoacetate (-3.98 kcal/mol) and pentalenolactone (-6.87 kcal/mol). In order to validate the docking results, compounds with structural similarities to lupane derivative 1, and 2 were isolated from *Baillonella toxisperma* (Pierre), modified and evaluated against *Plasmodium falciparum* 3D7 strains.
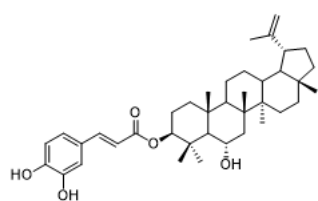
3β-caffeoyloxy-lup-20(29)-en-6α-ol (1)   3β-O-(E)-3,5-dihydroxycinnamoyl-olean-12-en-11-one (2)

In this study, a series of lupane derivatives were designed, isolated, synthesized and evaluated for antiplasmodial activity against *Plasmodium falciparum*.

Results And Discussion

2.1. Chemistry

2.1.1. Extraction, isolation and characterization

Plant material

The stem bark and leaves of *Baillonella toxisperma* was harvested in Bôt-Makak, in the Centre Region of Cameroon in May 2021 and authentication done at the National Herbarium in Yaounde, Cameroon by Mr Nana Victor (Botanist at National Herbarium in Yaounde, Cameroon) where a voucher specimen (14592 SRF/Cam) has been deposited.

Extraction and isolation of triterpenoids

7 kg of *Baillonella toxisperma* stem bark was air-dried, powdered and extracted using a sonicator at room temperature in methylene chloride-methanol (5 x 5 L) for 3 days. Filtration and concentration in a rotary evaporator afforded an oily reddish-brown extract (330 g). The crude extract (300 g) was fixed on silica

gel (300 g) and subjected to flash chromatography on silica gel (200 g) eluting with *n*-hexane, Hex/CH$_2$Cl$_2$ (1:1), CH$_2$Cl$_2$/AcOEt (1:1), CH$_2$Cl$_2$/MeOH (1:1) and MeOH respectively to provide five main fractions. Fraction 1 (15 g, obtained with pure hexane) was subjected to further separation by column chromatography on silica gel (75 g), with a step-wise gradient of gradients of EtOAc in hexane as mobile phase, to yield 25 mg of olean-12-en-3β-hexadecanoate (3) [11] and 40 mg of 3-β-*trans* cinnamoyloxylup-20(29)-ene (4) [12] after recrystallisation in Hexane. Fraction 2 (14.8 g obtained with Hex/CH$_2$Cl$_2$ [1:1]) was fixed and chromatographed on a silica gel column eluted with increasing polarities of EtOAc and hexane to yield 5 mg of compound 3-β-*trans* cinnamoyloxylup-20(29)-ene (4) and 5 mg of oleanoic acid benzoate (5) [13]. Fraction 3 (55 g obtained with CH$_2$Cl$_2$/AcOEt [1:1]) was subjected to silica gel column chromatography and eluted with increasing polarities of EtOAc and hexane to yield 5 mg of 3β-amyrin (6) [14], 6 mg of taraxerol (7) [15], 25 mg of betulonic acid (8) [16], 50 mg of β-sitosterol (9) [17], 50 mg of betulinic acid (10) [18], 25 mg of 3β-(*trans-p*-Coumaroyl)oxylup-20(29)-en-28-oïc acid (11) [18]. Fraction 4 (12.9 g obtained with CH$_2$Cl$_2$/MeOH [1:1]) was fixed and chromatographed on a silica gel column eluted with varying proportions of EtOAc and hexane to yield 25 mg of compound 10 and 5 mg of compound 11 (Figure 1).

Betuline (12) [16] with similar lupane scaffold and oleanolic acid (13) [19] previously isolated in our laboratory from *Alstonia scholaris* were also evaluated for structure activity relation (SAR) studies (Figure 1).

2.1.2 Chemical transformations

To discover derivatives with structure-diversities, we introduced the privilege medicinal structure with α-β unsaturated carbonyl functions to our lupane scaffold, which led to the discovery of new lupane derivatives that possesses favorable anti-malarial efficacies against *P. falciparum* 3D7 strains.

The derivatives 14-19 were all obtained as white solids from silica gel column chromatographic purification by gradient elution using hexane/ethyl acetate. Their molecular formula were determined by LC-MS (APCI$^+$).

Their ^{1}H NMR spectrum (500 MHz, CDCl$_3$ or DMSO-d$_6$) exhibited signals indicative of aldehyde protons at δ$_H$ = 9.50 (1H, s) and two down field terminal olefin protons at δ$_H$ = 5.95 (1H, d) and δ$_H$ = 6.30 (1H, d) and the disappearance of methyl-30 at δ$_H$ = 1.59 (3H, s).

Their ^{13}C NMR spectrum (125 MHz, CDCl$_3$ or DMSO-d$_6$) exhibited signals for a carbonyl atom at δ$_C$ = 196.0 (CHO) and the disappearance of methyl carbon at δ$_C$ = 18.2 (CH$_3$-30).

However, the appearance of α, β-unsaturated olefin peaks were not observed on the ^{13}C NMR spectrum. The presence of these peaks at δ$_C$ = 134.6 and δ$_C$ = 156.8 were made evidence thanks to their HSQC and HMBC spectra.

The disappearance of these peaks during ^{13}C NMR measurements maybe due to the inability of these bonds come into resonance due to the anisotropic effect of the carbonyl function.

The structures of the synthesized compounds were confirmed from the interpretation of their 1D and 2D NMR spectral data (Table 2).

Table 2: ^{1}H and ^{13}C NMR spectral data of the synthesized compounds

2.2. Biological activity

The isolated compounds and the new lupane derivatives 14, 15, 16, 17, 18 and 19 were evaluated against *P. falciparum*. Their percent growth inhibitions at 10 µM and half maximal inhibitory concentrations are reported in Table 3. The results indicated that the SeO$_2$ derivatives were more potent than their initial derivatives with compound 14 being the most active with an IC$_{50}$ of 0.703 µM.

Table 3: Antiplasmodial activity results with more active compounds in red

N°	δ_C (DEPT) 14	δ_H (m, J in Hz) 14	δ_C (DEPT) 15	δ_H (m, J in Hz) 15	δ_C (DEPT) 16	δ_H (m, J in Hz) 16	δ_C (DEPT) 17	δ_H (m, J in Hz) 17	δ_C (DEPT) 18	δ_H (m, J in Hz) 18	δ_C (DEPT) 19
1	39.6(CH_2)	0.99(m);1.67(br d, J= 12.9Hz)	38.8(CH_2)	0.92(m);1.57(br d, J= 12.0Hz)	38.2(CH_2)	0.99(m);1.67(brd, J= 12.8Hz)	38.2(CH_2)	1.09(m);1.71(br d, J= 13.0Hz)	38.2(CH_2)	0.99(m);1.67(br d, J= 12.9Hz)	38.2(
2	34.1(CH_2)	1.85(m)	27.4(CH_2)	1.47(m);1.72(dd, 10 and 12Hz)	34.2(CH_2)	1.85(m)	34.2(CH_2)	1.88(m)	34.2(CH_2)	1.85(m)	
3	218.1(C)	-	77.22(CH)	2.97 (dd, 5 and 10Hz)	81.0(CH)	4.43 (m)	78.8(CH)	4.63 (dd)	77.3(CH)	3,24 (m)	78.8(
4	47.3(C)	-	38.3(C)	-	38.3(C)	-	38.3(C)	-	38.9(C)	-	38.3(
5	54.9(CH)	0.82(m)	55.3(CH)	0.72(m)	55.4(CH)	0.82(m)	55.4(CH)	0.82(m)	55.4(CH)	0.82(m)	55.4(
6	19.6(CH_2)	1.56(m); 1.38(m)	18.3(CH_2)	1.55(m); 1.33(m)	18.1(CH_2)	1.56(m); 1.38(m)	18.1(CH_2)	1.56(m); 1.38(m)	18.4(CH_2)	1.56(m); 1.38(m)	18.1(
7	33.6(CH_2)	1.45(m); 1.38(m)	34.3(CH_2)	1.44(m); 1.38(m)	34.2(CH_2)	1.45(m); 1.38(m)	34.2(CH_2)	1.45(m); 1.38(m)	34.4(CH_2)	1.45(m); 1.38(m)	34.2(
8	40.7(C)	-	41.0(C)	-	40.6(C)	-	40.6(C)	-	40.6(C)	-	40.6(
9	49.9(CH)	1.38(m)	50.1(CH)	1.38(m)	50.37(CH)	1.38(m)	50.37(CH)	1.38(m)	50.3(CH)	1.38(m)	50.37
10	37.0(C)	-	37.4(C)	-	37.0(C)	-	37.0(C)	-	37.2(C)	-	37.0(
11	21.4(CH_2)	1.43(m); 1.21(m)	20.9(CH_2)	1.42(m); 1.22(m)	20.8(CH_2)	1.43(m); 1.21(m)	20.8(CH_2)	1.43(m); 1.21(m)	20.9(CH_2)	1.43(m); 1.21(m)	20.8(
12	25.5(CH_2)	1.21(m); 1.94(m)	25.6(CH_2)	1.23(m); 1.91(m)	25.4(CH_2)	1.21(m); 1.94(m)	25.4(CH_2)	1.21(m); 1.94(m)	25.4(CH_2)	1.21(m); 1.94(m)	25.4(
13	38.5(CH)	2.58(m)	37.0(CH)	2.74(m)	37.9(CH)	2.74(m)	37.9(CH)	2.74(m)	37.9(CH)	2.74(m)	37.9(
14	42.5(C)	-	42.8(C)	-	42.3(C)	-	42.3(C)	-	42.4(C)	-	42.3(
15	30.5(CH_2)	1.26(m); 1.88(m)	27.1(CH_2)	1.26(m); 1.88(m)	30.5(CH_2)	1.26(m); 1.88(m)	30.5(CH_2)	1.26(m); 1.88(m)	30.5(CH_2)	1.26(m); 1.88(m)	30.5(
16	32.1(CH_2)	1.55(m); 2.63(m)	29.3(CH_2)	1.55(m); 2.63(m)	32.2(CH_2)	1.55(m); 2.63(m)	32.2(CH_2)	1.55(m); 2.63(m)	32.2(CH_2)	1.55(m); 2.63(m)	32.2(
17	56.3(C)	-	47.8(C)	-	56.2(C)	-	56.2(C)	-	56.0(C)	-	56.2(
18	49.2(CH)	1.77(t, J=11.5Hz)	47.8(CH)	1.77(m)	46.9(CH)	1.77(t, J=11.5Hz)	46.9(CH)	1.70(m)	46.9(CH)	1.77(t, J=11.5Hz)	46.9(
19	46.8(CH)	2.74(m)	48.(CH)	2.65 (m)	49.1(CH)	3.52(m)	49.1(CH)	3.52(m)	49.1(CH)	3.52(m)	49.1(
20	147.3(C)	-	148.3(C)	-	150.6(C)	-	41.1(CH)	1.40(m)	147.3(C)	-	150.9
21	29.7(CH_2)	1.53(m); 2.24(m)	29.8(CH_2)	1.53(m); 2.24(m)	29.5(CH_2)	1.53(m); 2.24(m)	29.5(CH_2)	1.53(m); 2.24(m)	29.6(CH_3)	1.53(m); 2.24(m)	29.5(
22	37.0(CH_2)	1.57(m); 2.25(m)	34.0(CH_2)	1.56(m); 2.15(m)	37.0(CH_2)	1.57(m); 2.25(m)	37.0(CH_2)	1.57(m); 2.25(m)	36.6(CH_3)	1.57(m); 2.25(m)	37.0(
23	26.6(CH_3)	1.27 (s)	28.0(CH_3)	0.88 (s)	27.8(CH_3)	0.98 (s)	28.0(CH_3)	0.96(s)	27.6(CH_3)	0.86 (s)	28.0(
24	21.0(CH_3)	1.09 (s)	15.3(CH_3)	0.66 (s)	15.7(CH_3)	0.94 (s)	16.2(CH_3)	1.05(s)	16.1(CH_3)	0.66 (s)	16.2(
25	16.0(CH_3)	0.95 (s)	16.1(CH_3)	0.76 (s)	15.9(CH_3)	0.90 (s)	16.7(CH_3)	0.91(s)	16.2(CH_3)	0.76 (s)	16.7(
26	15.8(CH_3)	1.01 (s)	16.1(CH_3)	0.91 (s)	16.4(CH_3)	0.88 (s)	17.8(CH_3)	0.89(s)	16.4(CH_3)	0.87 (s)	17.8(
27	14.6(CH_3)	0.99 (s)	14.7(CH_3)	0.98 (s)	14.5(CH_3)	0.87 (s)	15.9 (CH_3)	0.85(s)	14.8(CH_3)	0.91 (s)	15.9
28	180.9(C)	-	58.23(CH_3)	3.53 and 3.09 (d, 10 Hz)	179.0(C)	-	179.0(C)	-	177.6(C)	-	14.4
29		6.30 and 5.94 (br s)		6.42 and 6.08 (br s)		6.47and 6.10(br s)		3.33(m); 3.58(m)		6.47 and 6.10 (s)	
30	105.8(CH_2)	9.50 (s)	105.8(CH_2)	9.51 (s)	109.3(CH_2)	9.53 (s)	55.3(CH_2)	0.94(s)	105.8(CH_2)	9.50 (s)	110.7
1'	198.2(C)		196.0(C)		198.0(CH)	-	15.1(CH_3)	-	196.0(C)		195.3

Position			
2′	167.8(C)	6.15 (d, J= 15 Hz)	166.8
3′	115.0(CH)	7.48 (d, J= 15 Hz)	119.1
1″	144.6(CH)		144.5
2″	125.96(C)	-	134.8
3″	129.8(CH)	6.72 (d, J= 5 Hz)	129.1
4″	115.7(CH)	7.31 (d, J= 5Hz)	128.2
5″	159.3(C)		130.3
6″	115.7(CH)	-	128.2
	129.8(CH)	7.31 (d, J= 5 Hz)	129.1
		6.72 (d, J= 5 Hz)	

Compounds	% growth inhibition	IC$_{50}$ Pf 3D7 (μM)
3	11.92	NA
4	7.99	NA
5	22.00	NA
6	0.00	NA
7	19.39	NA
8	100.00	3.88
9	53.50	NA
10	40.14	NA
11	100.00	1.38
12	0.00	NA
13	14.47	NA
14	99.45	0.703
15	98.38	2.15
16	100	1.28
17	79.8	≥ 10
18	98.28	3.79
19	15.4	NA
ART	NA	12.9

NA= not active

ART= Artemisinin

Conclusion

In summary, to develop potent anti-malaria agents based on lupane skeleton with better metabolic stabilities, we have designed, isolated, synthesized a series of lupane derivatives and evaluated their anti-malaria efficacies against *Plasmodium falciparum* 3D7 strains. The carbonyl group or 4-hydroxy cinamate group at position 3 of the lupane structure may greatly have an influence in the biological activities. The derived compounds with α-β unsaturated carbonyl motive show favorable antiplasmodial activities. In particular, compound 8 with % growth inhibition and IC$_{50}$ values of 100 and 3.88 μM when transformed to compound 14 showed % growth inhibition and IC$_{50}$ values of 100 and 0.703 μM respectively. Compound 11 also with % growth inhibition and IC$_{50}$ values of 100 and 1.38 μM when transformed to compound 16 showed % growth inhibition and IC$_{50}$ values of 100 and 1.28 μM respectively. Smaller concentrations of the derived compounds with α-β unsaturated carbonyl motive are needed to produce 100 % growth inhibition. These compounds will further be studied for subsequent mode of action study.

Experimental

General experimental procedures

Melting points were performed on a Büchi SMP-20 melting point apparatus. The NMR spectra in chloroform-d and methanol-d_4 were obtained using Brucker BioSpin GmbH instruments, operating at 400 MHz for ^{1}H NMR and 100 MHz for ^{13}C NMR. Chemical shifts are given in δ (ppm) using tetramethylsilane (TMS) as internal standard. EI-MS was obtained with JEOL JMS-600H mass spectrometer. The extraction of the plant material was done using a digital ultrasonic cleaner LMUC series of mark LABMAN (serial number L1328). Flash chromatography was performed on SCHOTT Buchner (Duran, West Germany) with a porosity of 4. Analytical thin-layer chromatography (TLC) was performed on precoated silica gel plates (Merck 60F$_{254}$; 20x20, 0.25 mm). Column chromatography was performed on silica gel (70-230 mesh; Merck). Chromatograms were visualized by spraying with a solution of 10 % H_2SO_4, iodine vapor or under ultraviolet light of wavelengths 254 and 366 nm.

Molecular docking studies

Preparation of Ligand

4000 compounds were selected from the CANAPL database and distributed in 39 classes namely Alkane, Alcohol, Alkaloid, Amide, Anthranol, Enthrone, Aromatic compounds, Benzophenone, Carotenoids, Ceramide, Cerebroside, Chromone, Coumarin, Cyanogenic glycoside, Cyclitol (polyol), Depsidone, Endiandric acid, Fatty acid, Flavonoid, Ionone, Iridoid, Labdane, Lactone, Lignane, Limonoid, Monoterpene, Peptide cyclic, Pterocarpans, Pyrone, Quinone, Sesquiterpene lactone, Saponins, Sesquiterpenoid, Sphingolipid, Steroid, Stilbenes, Sugar, Tannin, Terpenoids and Xanthone. The 3D structures of the phytoconstituents were retrieved from our chemical database and saved in .pdb format using Chem3D 15.0. The ligands were imported to the workspace and preparation was done for docking studies. The docking results of different constituents were compared against the reference drugs (heptelidic acid, iodoacetate and pentalenolactone) [21, 22] obtained from the drug bank in chemdraw (*cdx) format.

Preparation of Enzyme

The target for docking studies selected was Glyceraldehyde 3-phosphate dehydrogenase. Docking analysis was done by initially selecting the target for the disease and followed by obtaining the 3D structure of Glyceraldehyde 3-phosphate dehydrogenase (1ywg) [23] from protein data bank in .pdb format.

The AutoDockTools [24] (ADT) was used to prepare the ligand and receptor structures, add appropriate Gasteiger and Kollman charges, identify and modify ligand rotatable bonds. The potential binding sites of target were calculated using the Lamarckian GA (4.2) algorithm implemented in Autodock4 [25]. The population size, maximum number of evaluation (medium) and maximum number of generations were set at 150, 27 000 and 2 500 000 respectively [26]. The search space of the simulation exploited in the docking studies was studied as a subset region of 0.375Å around the active site [27]. The water molecules were removed from the enzyme to decrease interactions between functional group of ligands and water molecules.

Parameters for docking functions

At this time, more than 30 molecular docking programs are available. The commonly used are AutoDock [28], GOLD, FlexX, DOCK and ICM. According to Sousa et al., [29] we performed in-silico docking analysis by using Autodock4.0 [28]. This software uses two programs:

AutoGrid program calculates the interactions cards of grid in order to maximize evaluation step of different configurations of ligands. A grid surrounds the receptor protein and the ligand is placed at each intersection. The energy of interaction of this molecule with the protein is calculated and assigned to the location of the probe atom on the grid. An affinity grid is calculated for each type of ligand atom. The energy calculation time using the grids is proportional to the number of atoms of the ligand but it's independent of the number of atoms in the enzyme.

AutoDock program performs the research and evaluation of the different ligand configurations. It is possible to use several techniques to obtain the configurations (by simulated annealing, genetic algorithm or by Lamarckian genetic algorithm).

A grid-based method was used to enhance the quick evaluation of the binding energy of conformations of the complexes formed. The grid boxes were centered using coordinates of a virtual center of mass atom for the enzymes [3]. A grid box had dimensions of 44 Å × 44 Å × 58 Å respectively in x, y and z dimension according to amino acids which formed active site (Cys153 - His180). The affinity of the docked complexes was described using dissociation constants (K_i) (Equation (1)), binding energy based on the semi empirical force field expression as described in Equation (2) [30] and H-Bond interactions.

$$K_i = Exp(-\Delta G/RT) \qquad (1)$$

Where K_i (dissociation constant, and i indicates it is also an inhibition constant)

$$\Delta G_{bind} = \Delta G_{vdw} + \Delta G_{hbond} + \Delta G_{elect} + \Delta G_{tor} + \Delta G_{desolva} \qquad (2)$$

ΔG_{bind}	Free Energy of Binding
ΔG_{vdw}	Van der Waals potential
ΔG_{hbond}	Hydrogen bonding potential
ΔG_{elect}	Electrostatic Potential
ΔG_{tor}	Torsional energy
$\Delta G_{desolva}$	Free Energy of desolvation

Synthesis

Procedure for the oxidation of some triterpenoids with selenium oxide SeO$_2$

To a dry DCM or Dioxane solution of the olefin in a 100 mL conical flask, SeO$_2$ was added (1.5 eq) at room temperature. The reaction mixture was refluxed while stirring for 1-3 h. After partial evaporation of the solvent to reduce the volume of the mixture, the residue was fixed to silica gel and submitted to column chromatography using Hex/AcOEt in various proportions.

Betulonic acid acrylaldehyde 14: white solid (CH$_2$Cl$_2$); (Hex/AcOEt 18%); mp 182°C; yield: 30%; ^{1}H NMR (CDCl$_3$, 500 MHz): δ = 9.50 (1H, s, H-30), δ = 6.30 and 5.94 (each 1H, br s, H-29), 1.27 and 1.09 (each 3H, 2XCH$_3$), 1.01-0.99 (6H, s), 0.95 (3H, s, CH$_3$); ^{13}C NMR (CDCl$_3$, 125 MHz): δ = 218.1 (C, C-3), δ = 198.2 (C, C-30), 180.9 (C, C-28), 147.3 (C, C-20), 105.8 (CH$_2$, C-29).

Betuline acrylaldehyde 15: white solid (CH$_2$Cl$_2$/MeOH); (Hex/AcOEt 27%); mp 258 °C; yield: 30%; ^{1}H NMR (CDCl$_3$, 500 MHz): δ = 9.51 (1H, s, H-30), δ = 6.31 and 5.93 (each 1H, br s, H-29), 1.27 and 1.09 (each 3H, 2XCH$_3$), 1.01-0.99 (6H, s), 0.95 (3H, s, CH$_3$); ^{13}C NMR (CDCl$_3$, 125 MHz): δ = 198.4 (C, C-30), 180.9 (C, C-28), 148.3 (C, C-20), 105.8 (CH$_2$, C-29), δ = 79.01 (C, C-3).

3β-(*trans-p*-Coumaroyl)oxylup-20(29)-en-28-oïc acid acrylaldehyde 16: white solid (CH$_2$Cl$_2$/MeOH); (Hex/AcOEt 28.5%); mp 300 °C; yield: 30%; ^{1}H NMR (CDCl$_3$, 500 MHz): δ = 9.53 (1H, s, H-30), δ = 7.48 (1H, d, J = 15.0 Hz, H-3'), 7.31 (2H, d, J = 5.0 Hz, H-3", H5"), 6.72 (2H, d, J = 5.0 Hz, H-2", H-6"), 6.15 (1H, d, J = 15.0 Hz, H-2'), 6.47 and 6.10 (each 1H, br s, H-29), 4.43 (1H, m, H-3α), 0.98, 0.94, 0.90, 0.88 and 0.87 (each 3H, s, H-23, H-24, H-25, H-26 and H-27 respectively).

30-hydroxy betulinic acid 17: white solid (CH$_2$Cl$_2$/MeOH); (Hex/AcOEt 21%); mp 250 °C; yield: 25%; ^{1}H NMR (CDCl$_3$, 500 MHz): δ = 4.14 (1H, dd, H-3), 3.20-2.80 (2H, dd, H-30), 0.88 (3H, d, J = 10Hz, H-29), 0.87, 0.86 and 0.85 (each 3H, s, 3xCH$_3$), 0.73 (3H, s, CH$_3$), 0.65 (3H, s, CH$_3$); ^{13}C NMR (CDCl$_3$, 125 MHz): δ = 179.1 (C, C-28), 78.8 (CH, C-3), 60.4 (CH$_2$, C-30).

Betulinic acid acrylaldehyde 18: white solid (CH$_2$Cl$_2$/MeOH); (Hex/AcOEt 23%); mp 284 °C; yield: 40%; ^{1}H NMR (CDCl$_3$, 500 MHz): δ = 9.55 (1H, s, H-30), δ = 6.31 and 5.94 (each 1H, br s, H-29), 3.20 (1H, m, H-3), 1.27 and 1.09 (each 3H, 2XCH$_3$), 1.01-0.99 (6H, s), 0.95 (3H, s, CH$_3$); ^{13}C NMR (CDCl$_3$, 125 MHz): δ = 194.9 (C, C-30), 180.9 (C, C-28), 147.3 (C, C-20), 105.8 (CH$_2$, C-29), δ = 78.9 (C, C-3).

(3β-*trans* cinnamoyloxylup-20(29)-ene) acrylaldehyde 19: white solid (CH$_2$Cl$_2$/MeOH); (Hex/AcOEt 6%); mp 180°C; yield: 30%; ^{1}H NMR (CDCl$_3$, 500 MHz): δ = 9.54 (1H, s, H-30), δ = 7.68 (1H, d, J = 15.0 Hz, H-3'), 7.54-7.40 (5H, m, H-2",H-3", H-4", H5", H-6"), 6.46 (1H, d, J = 15.0 Hz, H-2'), 6.32-5.95 (each 1H, br s, H-29), 4.63 (1H, m, H-3α), 0.96, 1.05, 0.91, 0.89, 0.85, 0.94 (each 3H, s, H-23, H-24, H-25, H-26, H-27 and H-28 respectively).

Biological activity

Plasmodium falciparum culture and growth inhibition assay

Plasmodium falciparum 3D7 (chloroquine-sensitive) strain was obtained from the Biodefense and Emerging Infections (BEI) Research Resources (Manassas, VA) and maintained using a modified Trager and Jensen method. Briefly, parasites were cultured in fresh O$^+$ human red blood cells at 3% (v/v) hematocrit in RPMI 1640 culture media containing glutamax and NaHCO$_3$ (Gibco, UK), supplemented with 25 mM HEPES (Gibco, UK), 1X hypoxanthine (Gibco, USA), 20 µg/mL gentamicin (Gibco, China), and 0.5% Albumax II (Gibco, USA). When needed, parasites were synchronized at the ring stage by sorbitol treatment and cultured through one cycle before treatment.

Stock compound solutions were diluted in incomplete RPMI 1640 and mixed with parasite cultures (1% parasitemia and 1.5% hematocrit) in 96-well plates to a final drug concentration of 10 µM for hit identification studies, or 10 − 0.078 µM for activity confirmation assays. The final dimethyl sulfoxide (DMSO) concentration per 100 µL culture per well was 0.1%. Artemisinin at 1 µM was used as negative growth control, while the solvent treated culture (0.1% DMSO) was used as positive growth control. Following 72 h incubation at 37 °C, parasite growth was assessed by a SYBR green I-based DNA quantification assay. In brief, a 3X concentrated SYBR Green lysis buffer was added to each plate well containing parasitized erythrocytes and kept in the dark for about 30 minutes.

Fluorescence was measured using a Fluoroskan Ascent multi-well plate reader with excitation and emission wavelengths at 485 and 538 nm, respectively. Mean half-maximal inhibitory concentrations (IC_{50} values) were derived by plotting percent growth against log drug concentration and fitting the response data to a variable slope sigmoidal curve function using GraphPad Prism v8.0.

Declarations

Conflict of Interests: There are no conflicts of interest.

References

1. Kehr S, Sturm N, Rahlfs S, Przyborski JM, Becker K (2010) Compartmentation of Redox Metabolism in Malaria Parasites. PLoS Patho 6(12):1–12. https://doi:10.1371/journal.ppat.1001242
2. Guerra CA, Snow RW, Hay SI (2006) Defining the Global Spatial Limits of Malaria Transmission in 2005. Adv Parasit 62:157–179. https://doi:10.1016/S0065-308X(05)62005-2
3. Forlemu N, Watkins P, Sloop J (2017) Molecular Docking of Selective Binding Affinity of Sulfonamide Derivatives as Potential Antimalarial Agents Targeting the Glycolytic Enzymes: GAPDH, Aldolase and TPI. Open J Biophy 7(1):41–57. http://dx.doi.org/10.4236/ojbiphy.2017.71004
4. Plowe CV, Roper C, Barnwell JW, Happi CT et al (2007) World Antimalarial Resistance Network (WARN) III: Molecular Markers for Drug Resistant Malaria. Malar J 6(1):1–10. http://doi.org/10.1186/1475-2875-6-121
5. Bray PG, Barrett PM, Ward AS, De Koning PD (2003) Pentamidine Uptake and Resistance in Pathogenic Protozoa: Past, Present and Future. Trends Parasit 19(5):232–239. http://doi.org/10.1016/S1471-4922(03)00069-2
6. Verlinde CLMJ, Hannaert V, Blonski C, Willson M et al (2001) Glycolysis as a Target for the Design of New Anti-Trypanosome Drugs. Drug Resist 4(1):50–65. http://doi.org/10.1054/drup.2000.0177
7. Kim JW, Dang CV (2005) Multifaceted Roles of Glycolytic Enzymes. Trends Biochem Sci 30(3):142–150. http://doi.org/10.1016/j.tibs.2005.01.005
8. Seidler NW (2013) GAPDH and intermediary metabolism. Adv Experim Med Biol 985:37–59. http://doi.org/10.1007/978-94-007-4716-6_2
9. Ismail SA, Park HW (2005) ;D.61(11):1508–1513. http://doi.org/10.1107/S0907444905026740
10. Raeisi S (2013) Molecular docking studies of squalene synthase inhibitors as potential anti cardiovascular disease drugs: insights into drug–protein interaction discovery. Pharm Sci 19(2):39–44. http://pharm-sci.tbzmed.ac.ir
11. Chaudhuri K, Chawla HM (1987) Anthraquinones and terpenoids from Cassia javanica leaves. J Nat Prod 50(6):1183. http://doi.org/10.1021/np50054a035
12. Anjaneyulu V, Ravi K (1989) Triterpenoids from Mangifera indica. Phytochem 28(5):1695. http://doi.org/10.1016/S0031-9422(00)97767-7
13. Gwandu UZ, Dangoggo SM, Faruk UZ, Halilu, Yusuf AJ et al (2020) Isolation and Characterization of Oleanolic Acid Benzoate from the Ethylacetate Leaves Extracts of Vernonia ambigua (Kotschy Ex. Peyr). J Chem Soc Nigeria 45(5):1–6. http://doi.org/10.46602/jcsn.45i5.518
14. Bahuguna RP, Jangwan JS (1987) Puddumin-A, a new flavanone glucoside from Prunus cerasoides. J Nat Prod 50(2):309. http://doi.org/10.1021/np50050a020
15. Ogihara K, Higa M, Hokama K, Suga T (1987) Triterpenes from the leaves of Parsonia laevigata. Phytochem 26(3):783–785. http://doi.org/10.1016/S0031.9422(00)84786-X
16. Patra A, Chaudhuri SK, Panda SK (1988) Betulin-3-caffeate from Quercus suber, ^{13}C-nmr spectra of some lupenes. J Nat Prod 51(2):217–220. http://doi.org/10.1021/np50056a004
17. Chaturvedula VSP, Prakash I (2012) Isolation of stigmasterol and β-sitosterol from the dichoromethane extract of Rubus suavissimus. Int Cur Pharm J 1(9):239–242. http://doi.org/10.3329/icpj.v1i9.11613
18. Mbah JA, Zofou GND, Ngemenya MN, Efange SMN (2011) Antiplasmodial Triterpenes from the Stem Bark of *Baillonella Toxisperma*. ISESCO J Sci Tech 7(12):84–87
19. Shao CJ, Kasai R, Xu JDa, Tanaka O (1989) Saponins from leaves of Acanthopanax senticosus Harms., ciwujia. II.: structures of ciwujianosides A1, A2, A3, A4 and D3. Chem Pharm Bull 37(1):42–45. http://doi.org/10.1248/cpb.37.42
20. Eyong KO, Chinthapally K, Senthilkumar S, Lamshöft M, Folefoc GN et al (2015) Conversion of lapachol to lomatiol: synthesis of novel naphthoquinone derivatives. New J Chem 39(12):9611–9616. http://doi.org/10.1039/C5NJ01484K
21. Cane DE, Sohng J-K (1989) Inhibition of Glyceraldehyde-3-phosphate Dehydrogenase by Pentalenolactone: Kinetic and Mechanistic Studies. Arch Biochem Biophy 270(1):50–61. http://doi.org/10.1016/0003-9861(89)90006-4
22. Karja NWK, Fahrudin M, Kikuchi K (2009) Inhibitory Effect of Iodoacetate on Developmental Competence of Porcine Early Stage Embryos *In Vitro*. HAYATI J Biosc 16(1):25–29. http://doi.org/10.4308/hjb.16.1.25

23. Satchell JF, Malby RL, Luo CS, Adisa A et al (2005) Structure of glyceraldehyde-3-phosphate dehydrogenase from Plasmodium falciparum. Acta Crystallogr Sect D: Biol Crystallogr 61(9):1213–1221. http://doi.org/10.1107/S0907444905018317

24. Morris GM, Huey R, Lindstrom W, Sanner MF et al (2009) AutoDock4 and AutoDockTools4: Automated Docking with Selective Receptor Flexibility. J Comput Chem 30(16):2785–2791. http://doi.org/10.1002/jcc.21256

25. Bahadori MB, Dinparast L, Valizadeh H, Farimani MM et al (2016) Bioactive constituents from roots of Salvia syriaca L.: Acetylcholinesterase inhibitory activity and molecular docking studies. South Afr J Bot 106:1–4. http://dx.doi.org/10.1016/j.sajb.2015.12.003

26. Robien MA, Bosch J, Buckner FS, Van Voorhis WC et al (2006) Crystal structure of glyceraldehyde-3-phosphate dehydrogenase from Plasmodium falciparum at 2.25 A resolution reveals intriguing extra electron density in the active site. Proteins 62(3):570–577. http://doi.org/10.1002/prot.20801

27. Dhanik A, SMcMurray J, Kavraki L (2012) AutoDock based incremental docking protocol to improve docking of large ligands. IEEE Intern Conf Bioinfor Biomed Workshops (BIBMW) 48–55. http://doi.org/10.1109/BIBMW.2012.6470370

28. Sousa SF, Fernandes PA, Ramos MJ (2006) Protein-Ligand Docking: Current Status and Future Challenges. Proteins 65(1):15–26. http://doi.org/10.1002/prot.20802

29. Huey R, Morris GM, Olson AJ, Goodsell DSA (2006) Semi-Empirical Free Energy Force Field with Charge-Based Desolvation. J Comput Chem 28(6):1145–1152. http://doi.org/10.1002/jcc.20634

30. 30. Huey R, Morris GM, Olson AJ, Goodsell DSA. Semi-Empirical Free Energy Force Field with Charge-Based Desolvation. J Comput Chem. 2006;28(6):1145–1152. http://doi.org/10.1002/jcc.20634

Tables

Table 1 is available in the Supplemental Files section.
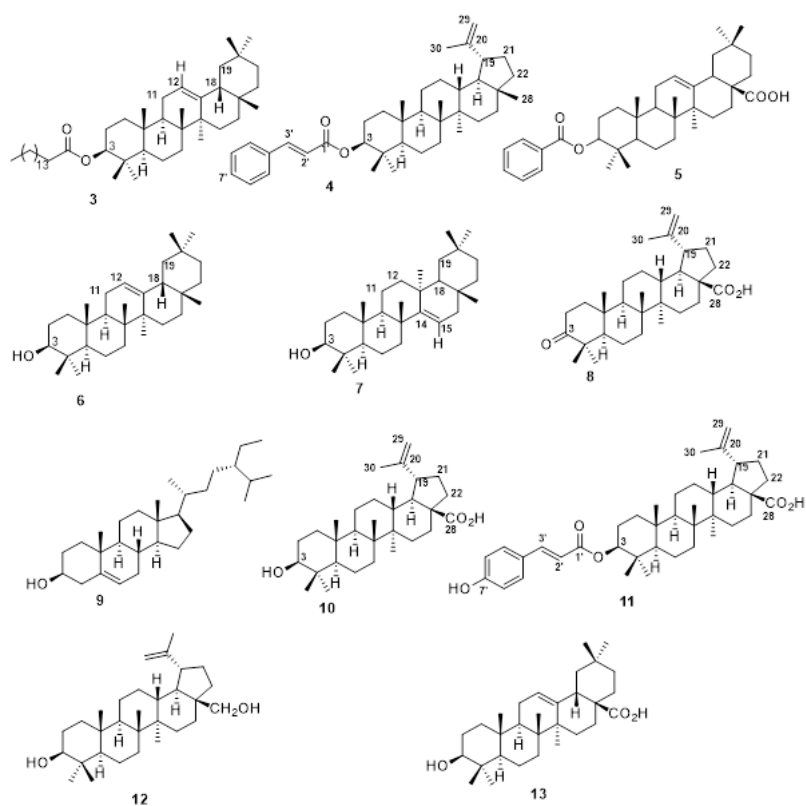
Figures

Figure 1

Structures of compounds isolated from *Baillonella toxisperma* (Pierre) including compounds 12 and 13

Supplementary Files

This is a list of supplementary files associated with this preprint. Click to download.

- Table1.docx

- SUPPORTINGINFORMATION24.04.22.docx